Langmuir

ARTICLE

pubs.acs.org/Langmuir

Comparative Height Measurements of Dip-Pen Nanolithography-Produced Lipid Membrane Stacks with Atomic Force, Fluorescence, and Surface-Enhanced Ellipsometric Contrast Microscopy

Michael Hirtz,[*,†] Rémi Corso,[*,‡] Sylwia Sekula-Neuner,[†] and Harald Fuchs[*,†,§]

[†]Institute of Nanotechnology (INT) and Karlsruhe Nano Micro Facility (KNMF), Karlsruhe Institute of Technology(KIT), Hermann-Von-Helmholtz-Platz 1, 76344 Eggenstein-Leopoldshafen, Germany

[‡]Nanolane, Parc des Sittelles, 72450 Montfort le Gesnois, France

[§]Westfälische Wilhelms-Universität and Center for Nanotechnology (CeNTech), Münster, Germany

Supporting Information

ABSTRACT: Dip-pen nanolithography (DPN) with phospholipids has been shown to be a powerful tool for the generation of biologically active surface patterns, but screening of the obtained lithographic structures is still a bottleneck in the quality control of the prepared samples. Here we performed a comparative study with atomic force microscopy (AFM), fluorescence microscopy (FM), and surface-enhanced ellipsometric contrast (SEEC) microscopy of phospholipid membrane stacks consisting of 1,2-dioleoyl-*sn*-glycero-3-phosphocholine (DOPC) with high admixing of 1,2-dipalmitoyl-*sn*-glycero-3-phosphoethanolamine-*N*-[6-[(2,4-dinitrophenyl)amino]hexanoyl] (DNP Cap PE) produced by DPN. We present a structural model of membrane stacking based on the combined information gained from the three microscopic techniques. Domains of phase-separated DNP Cap PE can be detected at high DNP Cap PE admixing that are not present at medium or low admixings. While the optical methods allow for a high-throughput screening of lithographic structures (compared to AFM), it was found that, when relying on FM alone, artifacts due to phase-separation phenomena can be introduced in the case of thin membrane stacks.

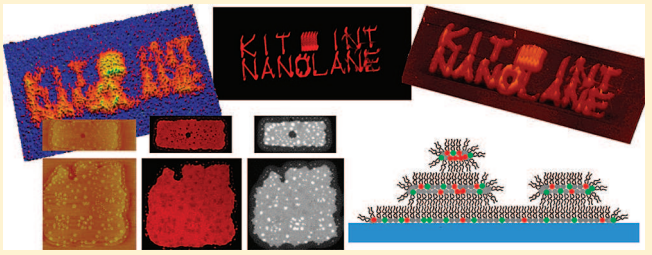

INTRODUCTION

Dip-pen nanolithography (DPN) was used to pattern phospholipids with a variety of admixings onto surfaces.[1,2] Due to the large area covered with patterns, quality control of prepared samples can become a bottleneck. When structural height and amount of deposited ink should be measured, atomic force microscopy (AFM) is generally the first choice. However, AFM is time-consuming for screening of large areas, which usually are prepared by DPN. Another recent approach is to admix a fluorescent probe into the phospholipid ink and determine the height of structures by fluorescence microscopy (FM).[3] It can be applied for thicker structures, but on thin ones within the order of only a few bilayers (below 10 nm), bleaching and phase separation may become an issue and the admixing of the fluorescent probe itself might introduce an unwanted additional component to the ink. Here we present a study on the characterization of a 1,2-dioleoyl-*sn*-glycero-3-phosphocholine (DOPC) membrane stack with high amounts of admixed 1,2-dipalmitoyl-*sn*-glycero-3-phosphoethanolamine-*N*-[6-[(2,4-dinitrophenyl) amino]hexanoyl] (DNP Cap PE), prepared by DPN, with AFM, FM, and SEEC microscopy.[4,5] Surface-enhanced ellipsometric contrast (SEEC) microscopy is based on the use of special microscope slides with an antireflective layer stacking for enhanced contrast of very thin films (down to 0.3 nm in height) in real time. SEEC microscopy was recently used to detect and study nano-objects such as nanometer-thin layers of peptides and proteins,[6−8] nanofluids,[9] or graphene sheets.[10] In addition to the contrast enhancement, 2D SEEC images can be turned into 3D maps through colorimetric correlation for complete topographic studies. 2,4-Dinitrophenyl (DNP) used in this study is a model allergen commonly used for the activation of immune cells in vitro and in vivo.[11,12] Ongoing studies in our lab utilize DNP Cap PE as a mean to immobilize DNP on surfaces to study the activation profiles of mast cells on lipid patterns with different concentrations of DNP or different pattern geometries. Therefore, we are interested in the properties of thin lipid membrane stacks with DNP Cap PE admixings, which would give insights into new properties of DNP-generated patterns. In the course of DPN with phospholipids, 1,2-dioleoyl-*sn*-glycero-3-phosphoethanolamine-*N*-(lissamine rhodamine B sulfonyl) (Liss Rhod PE) is routinely used as a fluorescent probe for large-scale monitoring of lithographic structures.

Received: July 14, 2011
Revised: August 3, 2011
Published: August 03, 2011

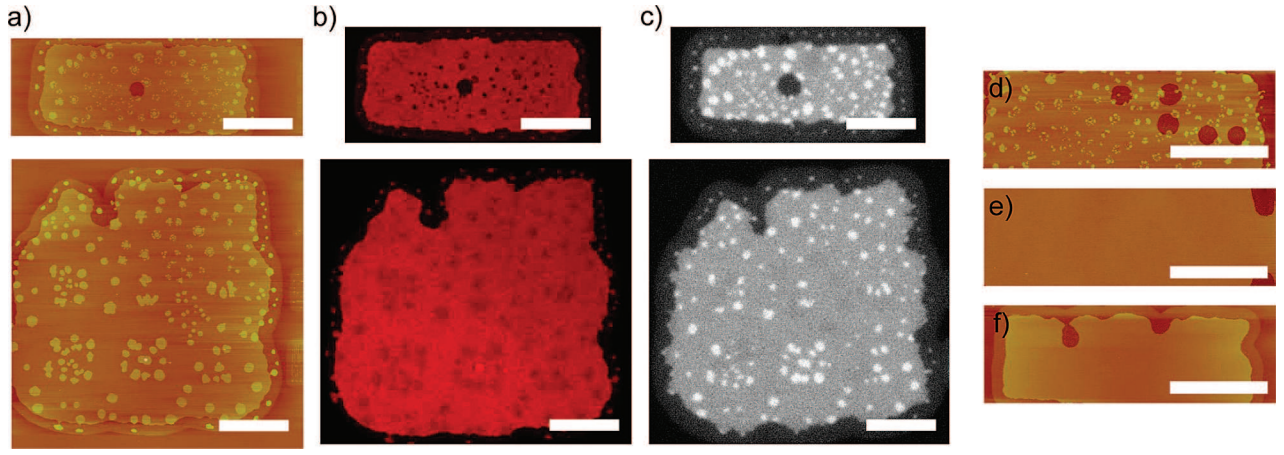

Figure 1. Images of two different lipid stack structures (top and bottom images) with 20 mol % admixing of DNP Cap PE to DOPC as carrier ink obtained by (a) AFM, (b) FM, and (c) SEEC microscopy. AFM micrographs of lipid stacks with (d) 20 mol %, (e) 10 mol %, and (f) no admixing of DNP Cap PE are also shown. All inks contained 1 mol % Liss Rhod PE. Scale bars = 20 μm.

MATERIALS AND METHODS

The phospholipids 1,2-dioleoyl-*sn*-glycero-3-phosphocholine (DOPC), 1,2-dioleoyl-*sn*-glycero-3-phosphoethanolamine-*N*-(lissamine rhodamine B sulfonyl) (18:1 Liss Rhod PE), and 1,2-dipalmitoyl-*sn*-glycero-3-phosphoethanolamine-*N*-[6-[(2,4-dinitrophenyl)amino]hexanoyl] (16:0 DNP Cap PE) were purchased from Avanti Polar Lipids, Inc. (structures are shown in Figure 3), and solutions of 1 mg/mL DOPC in HPLC-grade chloroform with admixings of 1 mol % Liss Rhod PE and 20 mol % DNP Cap PE were prepared. Inkwell chips (NanoInk, Inc.) were loaded with 3 μL of either DOPC/Liss Rhod PE or DOPC/DNP Cap PE/Liss Rhod PE solution, and type M-2 pen arrays (NanoInk, Inc.) were coated for 10 min at 70% relative humidity with those mixtures. Patterning was done with a DPN 5000 system (NanoInk, Inc.) on hydrophilic standard SURF samples (silicon oxide substrates with antireflective layering enabling SEEC; see Supporting Information, from Nanolane) at 48% humidity and 24 °C. The patterns were then inspected by fluorescence microscopy (Eclipse 80i, Nikon), AFM (Dimension Icon, Bruker) in tapping mode (aluminum-coated cantilever from Budget Sensors, 300 kHz resonance frequency, and 40 N/m spring constant), and SEEC microscopy (SARFUS 3D-AIR setup, Nanolane). Real-time visualization and measurements of DPN patterns were performed with Sarfusoft 2.4 3 D Premium software. All measurements were done in air under ambient conditions. The samples were checked by fluorescent microscopy before and after AFM to ensure pattern stability. Image processing for AFM images was done with onboard software and WSxM.[13]

RESULTS AND DISCUSSION

Typical membrane stacks prepared with 20 mol % admixing of DNP Cap PE to the DOPC carrier are shown in Figure 1a−c, inspected by (a) AFM, b) FM, and (c) SEEC microscopy.

AFM images indicate three different height levels of the lipid membrane stack. Interestingly, the third height level is only present in the case of high DNP Cap PE admixing (20 mol %) and is never observed on structures with lower or no DNP Cap PE admixing (Figure 1d−f), where only two height levels are observed. About 10% of the membrane stack area is covered with the third height features.

While correlating the features of the membrane stacks shown in Figure 1 with the images obtained by the different microscopy techniques, it becomes obvious that the highest features (third height level) visible in the AFM and SEEC images appear darker then the second height level in fluorescence. This indicates that the expectation "thicker membrane stack means higher fluorescence intensity" does not hold true for thin membrane stacks in the case of high-percentage admixings. Sections of one of the representative lipid membrane stacks of Figure 1 for the different imaging techniques are given in Figure 2 for detailed analysis.

For all three imaging techniques, four different heights and their respective intensity levels can be clearly distinguished. In the AFM we can identify these as (1) the flat silicon oxide surface of the sample, (2) a first lipid layer of approximately 1.3 nm thickness, (3) a second lipid layer of about 3.1 nm thickness, and (4) a third lipid layer with again 3.1 nm thickness. The thicknesses let us conclude that the first layer is a monolayer of lipids, whereas the second and third layer can be identified as lipid bilayers. The SEEC image profile shows optical thicknesses of 2.5 nm for the first layer, 5.0 nm for the second layer, and 4.8 nm for the third layer. A comparison of the different profiles indicates again that the third-level features appear darker in fluorescence although being clearly higher according to AFM and SEEC data. It must be noted that the fluorescence intensity drops almost to that of the single monolayer for the third-level structures; therefore the third-level domains have to influence also the second-level layer, otherwise there should be no drop in fluorescence intensity beyond that of the second-level layer. The fluorescence signal from the areas with the third-level layer domains is about 3.5 times lower than what would be expected if the third-level layer would give the same amount of extra intensity as the second-level layer. Since the third-level features and the accompanying drop in fluorescence intensity occur only in structures with high-level admixing of DNP Cap PE, a phase-separation phenomenon is likely to be the reason for it. Basically, two different scenarios could be responsible: (I) Phase separation of DNP Cap PE after reaching a certain concentration threshold leads to enrichment of DNP Cap PE in the third-level structure. A resulting phase transition in the third-level structures may influence also the areas under the structure itself to enrich the second-level layer with DNP Cap PE underneath the third-level layer domains (Figure 3a). The depletion in Liss Rhod PE leads to the drop in fluorescent intensity. To reach the observed drop in fluorescence intensity mentioned above (3.5 times less than expected), depletion to 0.3 mol % would be necessary. (II) Liss

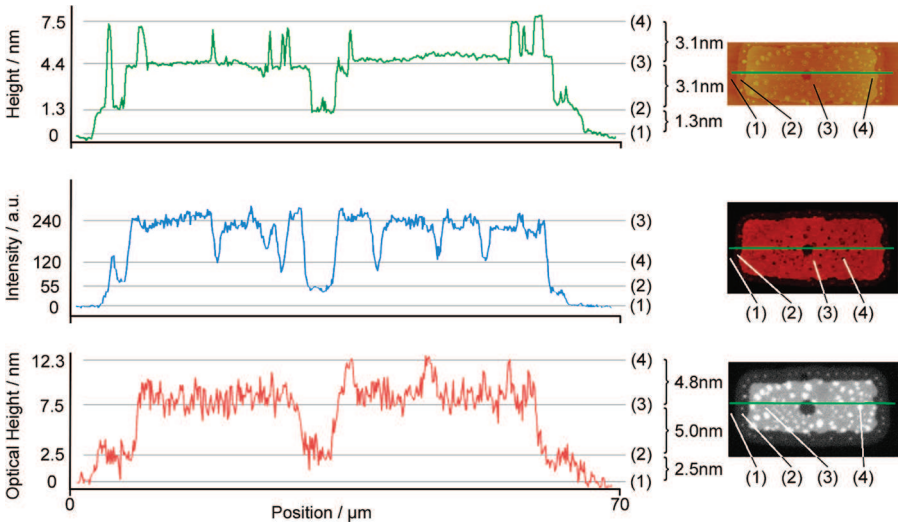

Figure 2. Profiles of the structure shown in top line of Figure 1 for AFM (top), FM (middle), and SEEC microscopy (bottom) images. The profile widths are approximately 70 μm. Insets mark the position where the section was taken (green line). Distinguishable and recurrent features are marked in the insets with numbers and the correspondent height levels are indicated with gray lines in the profiles: (1) sample surface, (2) first lipid layer (monolayer), (3) second lipid layer (bilayer), and (4) third lipid layer (bilayer).

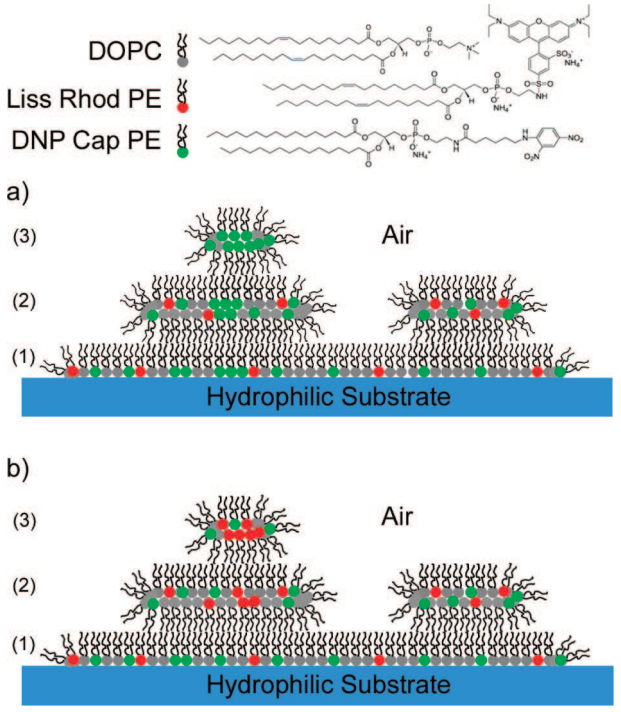

Figure 3. Structural model for lipid membrane stacking with 20 mol % DNP Cap PE admixing. The three-layer membrane stack consists of a single monolayer (1) as wetting layer and two bilayers (2, 3). Possible scenarios based on our observations are (a) an enrichment of DNP Cap PE in and under the third layer with decreased fluorescent intensity due to depleted Liss Rhod PE concentration or (b) an increased Liss Rhod PE concentration in and under the third layer causing self-quenching of the fluorophore.

Rhod PE itself is enriched in the third-level domains and the regions of the second-level membrane layer underneath the third-level domains by expulsion from the other membrane parts in the case of high DNP Cap PE admixing. The enrichment of Liss Rhod PE leads to self-quenching and a drop in fluorescence intensity. To account for the observed drop in fluorescence intensity (3.5 times less than expected), the Liss Rhod PE contents must rise to 4 mol % in the darkened areas.[14] Both scenarios could be possible, although we think scenario I is more likely because DNP Cap PE is in gel state at room temperature, in opposition to DOPC and Liss Rhod PE, which are already above their respective transition temperatures at room temperature and in liquid state [16:0 PE has a transition temperature of T_m = 63 °C, compared to T_m = −20 °C for DOPC and T_m = −16 °C for 18:1 (Δ9-Cis) PE (DOPE)].[15] Therefore, high amounts of admixing with DNP Cap PE should lead to phase separation of gel-state DNP Cap PE domains, while the fluid-state DOPC and Liss Rhod PE should be of better compatibility at room temperature.

Table 1. Thickness, Optical Thickness, and Calculated Refractive Index for Different Lipid Layers

layer[a]	thickness d,[b] nm	optical thickness d_o, nm	refractive index n[c]
1	1.3 ± 0.2	2.5 ± 0.4	1.92 ± 0.6
2	3.1 ± 0.2	5.0 ± 0.3	1.61 ± 0.5
3	3.1 ± 0.1	4.8 ± 0.2	1.55 ± 0.3

[a] The different lipid layers of the three-layered lipid membrane stacks were produced with 20 mol % admixing of DNP Cap PE into DOPC carrier ink. [b] From AFM data. [c] Based on eq 1.

Comparing the optical thickness obtained by SEEC microscopy with the physical thickness from AFM measurements gives us information about the refractive index of the different membrane stack layer. The optical thickness d_o is related to the physical thickness d by the refractive index n:

$$d_o = nd \quad (1)$$

Table 1 summarizes the physical thickness (from AFM data) and optical thickness (from SEEC data) as well as the resulting refractive index obtained from the measurements. The refractive indices, especially in the case of the monolayer, are higher than what would be expected from hydrated bilayers, although still in the range of some theoretical predictions.[16,17] Usually, fully

hydrated bilayers (i.e., under water) are regarded in experimental and theoretical approaches toward the refractive index of lipid bilayers. Therefore, we attribute the unusually high refractive index to the circumstance that in this experiment the bilayers are examined in air and ought to be more compact. This is also reflected in physical thicknesses that are a little bit smaller than what is measured in fully hydrated bilayers. The monolayer's refractive index is higher than that of the bilayers, indicating a raised density compared to the bilayers. The two bilayers have almost the same optical thickness; the slight decrease is an additional indication of the altered composition of the third membrane stack layer.

CONCLUSIONS

On the basis of the data obtained by different microscopic techniques (AFM, FM, and SEEC microscopy), we present a plausible scenario for the organization of the membrane stacking observed in lipid DPN-generated structures with high admixing of DNP Cap PE (Figure 3). Although fluorescence microscopy can speed up the screening process after the lithographic process step, it may lead to misinterpretations in the case of thin structures with high admixing of functional compounds as observed in this study. Phase-separation phenomena that lead to local concentration changes of the fluorescent probe molecules may hinder the identification of the stack structure or make it impossible to distinguish between domains or holes in the membrane stack. SEEC microscopy renders the fluorescent probe molecules unnecessary— which might be desirable for certain applications, since even small admixing of fluorescent probes can disturb membrane organization[18]—while still yielding fast information on stack packing that can easily hold up to the high-throughput pattern production by DPN, avoiding the bottleneck of AFM measurements. Most information on not-yet-characterized ink mixtures is obtained by a combination of all three approaches, using AFM for calibration purposes on a limited number of structures and the optical methods for routine screening and observation of phase-separation phenomena.

ASSOCIATED CONTENT

Supporting Information. Additional text and one figure with Information on the SURF substrate for SEEC microscopy. This material is available free of charge via the Internet at http://pubs.acs.org.

AUTHOR INFORMATION

Corresponding Author

*E-mail michael.hirtz@kit.edu (M.H.), remi.corso@eolane.com (R.C.), or fuchsh@uni-muenster.de (H.F.).

ACKNOWLEDGMENT

H.F. gratefully acknowledges support by the Deutsche Forschungsgemeinschaft within SFB 858 and the WCU program of the Korean Ministry of Education, Science and Technology at GIST/DNE, Gwangju, South Korea. This work was carried out with the support of the Karlsruhe Nano Micro Facility (KNMF, www.knmf.kit.edu), a Helmholtz Research Infrastructure at Karlsruhe Institute of Technology (KIT, www.kit.edu).

REFERENCES

(1) Lenhert, S.; Sun, P.; Wang, Y.; Fuchs, H.; Mirkin, C. A. *Small* **2007**, *3*, 71–75.
(2) Sekula, S.; Fuchs, J.; Weg-Remers, S.; Nagel, P.; Schuppler, S.; Fragala, J.; Theilacker, N.; Franzreb, M.; Wingren, C.; Ellmark, P.; Borrebaeck, C. A. K.; Mirkin, C. A.; Fuchs, H.; Lenhert, S. *Small* **2008**, *4*, 1785–1793.
(3) Nafday, O. A.; Lenhert, S. *Nanotechnology* **2011**, *22*, No. 225301.
(4) Ausserré, D.; Valignat, M.-P. *Opt. Express* **2007**, *15*, 8329–8339.
(5) Ausserré, D.; Valignat, M.-P. *Nano Lett.* **2006**, *6*, 1384–1388.
(6) Monot, J.; Petit, M.; Lane, S. M.; Guisle, I.; Léger, J.; Tellier, C.; Talham, D. R.; Bujoli, B. *J. Am. Chem. Soc.* **2008**, *130*, 6243–6251.
(7) Carion, O.; Souplet, V.; Olivier, C.; Maillet, C.; Medard, N.; El-Mahdi, O.; Durand, J.-O.; Melnyk, O. *ChemBioChem* **2007**, *8*, 315–322.
(8) Souplet, V.; Desmet, R.; Melnyk, O. *J. Pept. Sci.* **2007**, *13*, 451–457.
(9) Pauliac-Vaujour, E.; Stannard, A.; Martin, C.; Blunt, M.; Notingher, I.; Moriarty, P.; Vancea, I.; Thiele, U. *Phys. Rev. Lett.* **2008**, *100*, No. 176102.
(10) Vallés, C.; Drummond, C.; Saadaoui, H.; Furtado, C. A.; He, M.; Roubeau, O.; Ortolani, L.; Monthioux, M.; Pénicaud, A. *J. Am. Chem. Soc.* **2008**, *130*, 15802–15804.
(11) Orth, R. N.; Wu, M.; Holowka, D. A.; Craighead, H. G.; Baird, B. A. *Langmuir* **2003**, *19*, 1599–1605.
(12) Maier, J. V.; Brema, S.; Tuckermann, J.; Herzer, U.; Klein, M.; Stassen, M.; Moorthy, A.; Cato, A. C. B. *Mol. Endocrinol.* **2007**, *21*, 2663–2671.
(13) Horcas, I.; Fernández, R.; Gómez-Rodríguez, J. M.; Colchero, J.; Gómez-Herrero, J.; Baro, A. M. *Rev. Sci. Instrum.* **2007**, *78*, No. 013705.
(14) MacDonald, R. I. *J. Biol. Chem.* **1990**, *265*, 13533–13539.
(15) Information from data sheets provided by Avanti Polar Lipids, Inc.
(16) Oki, S. *J. Theor. Biol.* **1968**, *19*, 97–115.
(17) Huang, W.; Levitt, D. G. *Biophys. J.* **1977**, *17*, 111–128.
(18) Lapinski, M. M.; Blanchard, G. J. *Chem. Phys. Lipids* **2007**, *150*, 12–21.